UNCECOMP 2015
1st ECCOMAS Thematic Conference on
Uncertainty Quantification in Computational Sciences and Engineering
M. Papadrakakis, V. Papadopoulos, G. Stefanou (eds.)
Crete Island, Greece, 25–27 May 2015

SYSTEM IDENTIFICATION FOR UNCERTAINTY QUANTIFICATION IN AEROELASTIC PROBLEMS

Rakesh Sarma[1], **and Richard P. Dwight**[1]

[1]Delft University of Technology
The Netherlands
e-mail: R.Sarma@tudelft.nl

Keywords: Reduced Order Models, Uncertainty Quantification, Fluid Structure Interaction

Abstract. *Aeroelastic problems involve coupling of fluid and structural solvers to obtain the response of the system under a set of operating conditions. Unsteady aeroelastic phenomena such as flutter require the solution of these coupled equations for the entire flight regime and operating conditions. These coupled problems generally tend to be computationally intensive, primarily due to the fluid component. Uncertainties in structural parameters (due to e.g. manufacturing variability and fatigue) are important for determining the stability of the resulting system. The corresponding uncertain analysis requires many code runs, and can be computationally intractable. In this paper, we apply system identification to obtain a reduced-order model for the aerodynamic solver. This model is then coupled with the structural solver for obtaining the full aeroelastic solution.*

System identification is a data driven modeling approach for approximating a system based on input and observed outputs of the system. The resulting approximation is extremely cheap. We employ this to model the aerodynamic forces, given structural displacements, and these forces are exchanged with the structural solver to update the aeroelastic solution. Two ROMs are considered, AutoRegressive with eXogenous inputs (ARX), and a Linear Parameter Varying (LPV) model. The latter is expected to capture dynamics of the underlying system at multiple operating points.

A model is built and applied to 2-DoF airfoils. The obtained response for the 2-dimensional system is very much in agreement with the high-fidelity CFD solver. Results show that this data-driven approach can accurately predict the aerodynamic forces. With this technique, uncertainty in stability characteristics of the system can be rapidly estimated. An uncertainty quantification is performed by Monte-Carlo on the reduced order model.

1 Introduction

Fluid structure interaction (FSI) is observed in many physical systems such as aircraft and bridges. Under certain dynamic conditions, this interaction could lead to complete failure of the entire system. For example, it can cause structural failure of wings; hence having a direct impact on the loss of life. It occurs as a result of the dynamic interaction of fluid forces on the motion of a structure and vice versa. FSI analysis is required for aircraft certification to determine safe operating limits.

Both experimental and computational approaches exist for modeling FSI. Experimental FSI involves huge monetary investments, and aircraft manufacturers want to minimize the number of full scale tests through numerical simulations. Computational FSI offers challenges in terms of processing time due to the complexity of the system. It involves coupling fluid and structural solvers in time to obtain the full aeroelastic solution. Computationally, the structural solver is much faster than the fluid solver, resulting in simulation times dominated by the fluid part. This problem is further aggravated in high Reynolds number systems such as aircraft and wind turbines.

In this context, reduced order models (ROM) aim to reduce the computational time of the coupled system. The idea is to replace the fluid solver with a cheap ROM and perform a coupled solution of the structural solver with the ROM. ROMs can be broadly classified into projection-based and system identification-based methods. Both approaches approximate a high-fidelity model by reducing its dimension. In the case of projection-based method, this is achieved by construction of a low dimensional subspace onto which the continuous or discrete governing equations are projected, which results in a ROM. However the computational cost of assembling the low dimensional ROM scales with the large dimension of the underlying model [1].

In this paper, we present a system identification based ROM obtained by training of the model with high fidelity simulation data of the full system. System identification deals with the problem of building mathematical models of dynamical systems based on observed data from the system [2]. The accuracy of the trained model depends on the robustness of the training data and the model complexity. Typically power spectrum analysis of the training data is done to obtain the relative energy content in the signals. Signals with a wide frequency range are expected to lead to an accurate ROM. We consider an AutoRegressive with eXogenous (ARX) inputs model and a Linear Parameter Varying (LPV) ARX model with varying coefficients in order to study the effect of complexity on the robustness of our model. Section 2 gives the mathematical formulation of the ROMs implemented in this paper. The methodology for performing ROM based FSI is discussed in Section 3. In Section 4, FSI is performed by coupling this ROM with a structural solver for a 2-DoF airfoil. Finally, an uncertainty quantification problem is discussed in Section 5, with the implementation of the reduced aeroelastic solver.

2 ROM theory and formulation

2.1 ARX formulation

System identification techniques identify a mapping between the input and output of a system. The AutoRegressive with eXogenous inputs (ARX) model is based on a time marching procedure to predict the output of interest given previous observations and inputs which affect the system response. The assumption is of a low-dimensional linear model. Idea is to represent an underlying order differential equation with a discrete difference equation. System identifi-

cation concepts have been implemented for flutter prediction [3] and such techniques reported improvements in computational time [4][5]. This model can be represented mathematically with the linear difference equation:

$$z(t) = \sum_{i=1}^{n} a_i z(t-i) + \sum_{k=0}^{m_1} b_k^{(1)} d_1(t-k) + \cdots + \sum_{k=0}^{m_q} b_k^{(q)} d_q(t-k) + \epsilon_t. \tag{1}$$

Note that the output of interest z in (1) is estimated by the linear combinations of n 'past' observations of z and $d_i(i = 1, 2, \cdots, q)$ exogenous inputs. A least squares problem is solved to evaluate the coefficients a_i and $b_k^{(1)} \cdots b_k^{(q)}$ to minimize the error ϵ_t with respect to the input-output data obtained from the unsteady CFD solver. The accuracy of the approximation largely depends on the frequency content of the training signal with which the data is generated. The training signal should be chosen in such a manner that a broad frequency spectrum of the system is excited. In the current work, we apply chirp signals for training the ARX model. Chirp is a frequency sweep given by $\alpha = \alpha_o sin\big(\omega(t)t\big)$, where, α_o is the chirp amplitude and $\omega(t)$, e.g. $\omega(t) = \frac{\omega_1 - \omega_o}{t_1} t$, is known as the chirp rate with ω_1, ω_o and t_1 as the final frequency, start frequency and time step respectively. Frequency spectrum analysis is done to ascertain the energy content in the signals. The trained models are validated by reconstructing sinusoidal test signals in the training frequency regime. Based on the error estimates during reconstruction, the order of the model is optimized to improve accuracy of predictions.

2.2 LPV-ARX formulation

The ARX based system identification model discussed in the previous sections is a linear system with constant coefficients. The model can be trained under fixed operating conditions. But in practice, models valid over wider operating regimes are needed. In this context, we present a linear parameter varying (LPV) system in this section where the expansion coefficients are functions of a scheduling parameter. The LPV framework has been applied in diverse domains such as aerospace [6], process applications [7], wind industry [8]. Representation of the LPV model structure can be in the state-space form or input-output form. The LPV state space form has multiple strategies for identification such as gradient based methods [9], subspace approach[10]. Here, we adopt the input-output representation of the system, which results in a structure similar to ARX. It is based on a linear regression form [11, 12]:

$$z(t) = \sum_{i=1}^{n} a_i(p) z(t-i) + \sum_{k=0}^{m_1} b_k^{(1)}(p) d_1(t-k) + \cdots + \sum_{k=0}^{m_q} b_k^{(q)}(p) d_q(t-k) + \epsilon_t. \tag{2}$$

The expansion coefficients a_i and $b_k^{(j)}$ of the representation are not constants, but functions of some scheduling parameter $p(t)$ which is a function of time. The motivation for this representation is that the true system is not linear in practice. The LPV representation has similarities to gain scheduling approach, which is used in control systems. The approach in gain scheduling is to linearize the non-linear model at different operating points. The idea in LPV is to obtain a dynamic mapping between input and output which is dependent on the scheduling parameter. If only one exogenous input parameter is considered,(2) reduces to:

$$z(t) = \sum_{i=1}^{n} a_i(p) z(t-i) + \sum_{j=0}^{m} b_j(p) d(t-j) + \epsilon_t. \tag{3}$$

The expansion coefficients are assumed to be polynomials functions in p, which is a time-varying quantity:

$$\begin{aligned} a_i(p) &= a_i^1 + a_i^2 p + \cdots + a_i^N p^{N-1} \\ b_j(p) &= b_j^1 + b_j^2 p + \cdots + b_j^N p^{N-1} \end{aligned} \tag{4}$$

The coefficients can be represented in a matrix θ:

$$\theta \coloneqq \begin{bmatrix} a_1^1 & a_1^2 & \cdots & a_1^N \\ \vdots & \vdots & \ddots & \vdots \\ a_n^1 & a_n^2 & \cdots & a_n^N \\ b_0^1 & b_0^2 & \cdots & b_0^N \\ \vdots & \vdots & \ddots & \vdots \\ b_0^1 & b_0^2 & \cdots & b_0^N \end{bmatrix} \tag{5}$$

Now a matrix ψ_t is defined as the product of matrix ϕ_t containing 'past' input-output values and matrix of scheduling parameter polynomials π_t [11]. The subscript t denotes the value of the associated variable at time t, so that:

$$\psi_t \coloneqq \phi_t \pi_t \coloneqq \begin{bmatrix} -z_{t-1} \\ \vdots \\ -z_{t-n} \\ d_t \\ \vdots \\ d_{t-m} \end{bmatrix} \begin{bmatrix} 1 & p_t & p_t^2 & \cdots & p_t^{N-1} \end{bmatrix} \tag{6}$$

Equations (4) - (6) are substituted into (3) to obtain the solution at time t in the inner product form:

$$z_t = \langle \theta, \psi_t \rangle. \tag{7}$$

Note that the inner product $z_t = \langle \theta, \psi_t \rangle \coloneqq \text{trace}(\theta^* \psi_t) = \text{trace}(\psi_t \theta^*)$, where θ^* is the complex conjugate transpose of the matrix θ. The identification procedure is then based on forming a cost function for the estimate provided by (7). Let J be the cost function based on the square of the error in estimation,

$$\begin{aligned} J(\theta) &= \epsilon(t, \theta)^2 \\ \epsilon(t, \theta) &= \hat{z}_t - \langle \theta, \psi_t \rangle, \end{aligned} \tag{8}$$

where $\hat{z}_t$ is the true value at time t. The cost function is minimized to obtain the optimum value of the parameters. Note that the matrix π_t varies based on the requirement of operating conditions, thus providing the flexibility to take into account changes in field variables. In this work, the free stream wind velocity is considered as the scheduling parameter and the order of the polynomial $N = 5$. The obtained ROMs are then employed for performing FSI analysis. The formulation of the FSI problem is discussed in the next section.

3 ROM based FSI

In the current work, the coupling of flow and structural solvers is based on the Infinite Plate Spline (IPS) method developed by Harder and Desmarais [13]. The method is based on the

superposition of solutions obtained from the partial differential equations of an infinite plate. Further details of IPS can be found in the literature [13]. IPS identifies a linear relationship between the structural and fluid mesh. This map transforms the displacement from the structural to the fluid mesh. Subsequently the aerodynamic forces obtained at the fluid mesh points are transferred to the structural mesh applying the principle of virtual work.

The formulation for performing the stability analysis is based on the state space approach discussed in [4]. The structural equation considering damping and external aerodynamic forces is given by:

$$M\ddot{d} + C\dot{d} + Kd + z_w(t) = 0 \tag{9}$$

where $z_w(t)$ is the generalized aerodynamic load vector, M is the generalized mass matrix, C is the damping matrix, K is the stiffness matrix and d represents the displacement vector. The state space form of (9) is given by:

$$\begin{bmatrix} I & 0 \\ 0 & I \end{bmatrix} \begin{bmatrix} \dot{d} \\ \ddot{d} \end{bmatrix} - \begin{bmatrix} 0 & I \\ -M^{-1}K & -M^{-1}C \end{bmatrix} \begin{bmatrix} d \\ \dot{d} \end{bmatrix} - \begin{bmatrix} 0 \\ -M^{-1}z_w(t) \end{bmatrix} = 0 \tag{10}$$

or,

$$\dot{x_s}(t) = A_{st}x_s(t) + B_{st}z_w(t) \tag{11}$$

$$y_s(t) = C_{st}x_s(t) + D_{st}z_w(t) \tag{12}$$

where,

$$\begin{aligned} x_s(t) = \begin{bmatrix} d \\ \dot{d} \end{bmatrix} \qquad A_{st} = \begin{bmatrix} 0 & I \\ -M^{-1}K & -M^{-1}C \end{bmatrix} \\ B_{st} = \begin{bmatrix} 0 \\ -M^{-1} \end{bmatrix} \qquad C_{st} = \mathbf{I} \qquad D_{st} = 0 \end{aligned} \tag{13}$$

x_s is the state vector and y_s is the output vector. These continuous time equations are converted to the discrete form:

$$x_s(t+1) = G_s x_s(t) + H_s z_w(t) \tag{14}$$

$$y_s(t) = C_s x_s(t) + D_s z_w(t) \tag{15}$$

where, t is the current time and,

$$\begin{aligned} G_s = \mathrm{e}^{A_{st}\Delta t} \quad H_s = [\mathrm{e}^{A_{st}\Delta t} - \mathbf{I}][A_{st}^{-1}B_{st}] \\ C_s = C_{st} \qquad D_s = D_{st} \end{aligned} \tag{16}$$

The aerodynamic equation (1) is written for a single exogenous input as:

$$z_w(t) = \sum_{i=1}^{n}[A_i]z_w(t-i) + \sum_{i=0}^{m}[B_i]d(t-i) \tag{17}$$

where, d is the generalized displacement, z_w is the generalized aerodynamic force vector and n, m are known as the orders of the model. For the state space formulation of this model, a state vector x_w is defined for the time step t.

$$x_w(t) = \begin{bmatrix} z_w(t-1) \\ \vdots \\ z_w(t-n) \\ d(t-1) \\ \vdots \\ d(t-m) \end{bmatrix}. \tag{18}$$

The state space form of the aerodynamic equation can be written as:

$$x_w(t+1) = G_w x_w(t) + H_w d(t) \tag{19}$$

$$z_w(t) = C_w x_w(t) + D_w d(t) \tag{20}$$

where,

$$G_w = \begin{bmatrix} A_1 & A_2 & \dots & A_{n-1} & A_n & B_1 & B_2 & \dots & B_{m-1} & B_m \\ \mathbf{I} & 0 & \dots & 0 & 0 & 0 & 0 & \dots & 0 & 0 \\ 0 & \mathbf{I} & \dots & 0 & 0 & 0 & 0 & \dots & 0 & 0 \\ \vdots & \vdots & \ddots & \vdots & \vdots & \vdots & \vdots & \ddots & \vdots & \vdots \\ 0 & 0 & \dots & \mathbf{I} & 0 & 0 & 0 & \dots & 0 & 0 \\ 0 & 0 & \dots & 0 & 0 & 0 & 0 & \dots & 0 & 0 \\ 0 & 0 & \dots & 0 & 0 & \mathbf{I} & 0 & \dots & 0 & 0 \\ 0 & 0 & \dots & 0 & 0 & 0 & \mathbf{I} & \dots & 0 & 0 \\ \vdots & \vdots & \ddots & \vdots & \vdots & \vdots & \vdots & \ddots & \vdots & \vdots \\ 0 & 0 & \dots & 0 & 0 & 0 & 0 & \dots & \mathbf{I} & 0 \end{bmatrix} \quad H_w = \begin{bmatrix} B_0 \\ 0 \\ 0 \\ \vdots \\ 0 \\ \mathbf{I} \\ 0 \\ 0 \\ \vdots \\ 0 \end{bmatrix}$$

$$C_w = \begin{bmatrix} A_1 & A_2 & \dots & A_{n-1} & A_n & B_1 & B_2 & \dots & B_{m-1} & B_m \end{bmatrix} \quad D_w = B_0. \tag{21}$$

The output y_s of the structural equation (15) is to be fed as input to the aerodynamic equation after performing the transformation T given by IPS, which can be expressed as:

$$d(t) = T y_s(t) \tag{22}$$

The coupled structural and flow equations in state space form are required for the aeroelastic analysis to form a coupled matrix to ascertain the stability of the system. The aerodynamic equation in terms of the structural output can be written as:

$$x_w(t+1) = G_w x_w(t) + H_w T C_s x_s(t) \tag{23}$$

$$z_w(t) = C_w x_w(t) + D_w T C_s x_s(t) \tag{24}$$

Now the aerodynamic force is applied to the structural equation to obtain the displacements for the next time step. The forces require transformation for applying in the structural grid given by the transpose of T. Putting (23) and (24) in (14) and (15):

$$\begin{aligned} x_s(t+1) &= G_s x_s(t) + H_s T^T C_w x_w(t) + H_s T^T D_w T_w C_s x_s(t), \\ &= (G_s + H_s T^T D_w T_w C_s) x_s(t) + H_s T^T C_w x_w(t). \end{aligned} \tag{25}$$

The coupled form of equations is expressed in matrix form as:

$$\begin{bmatrix} x_s(t+1) \\ x_w(t+1) \end{bmatrix} = \begin{bmatrix} G_s + H_s T^T D_w T_w C_s & H_s T^T C_w \\ H_w T_w C_s & G_w \end{bmatrix} \begin{bmatrix} x_s(t) \\ x_w(t) \end{bmatrix}, \tag{26}$$

$$y_s(t) = \begin{bmatrix} d(t) \\ \dot{d}(t) \end{bmatrix} = \begin{bmatrix} C_s & 0 \end{bmatrix} \begin{bmatrix} x_s(t) \\ x_w(t) \end{bmatrix}. \tag{27}$$

Let the matrix formed in equation (26) be denoted by:

$$J_{sw} = \begin{bmatrix} G_s + H_s T^T D_w T_w C_s & H_s T^T C_w \\ H_w T_w C_s & G_w \end{bmatrix}. \tag{28}$$

The stability of this system is given by the stability theory for discrete linear systems. If λ is an eigenvalue of the matrix J_{sw}, then the system is stable if $\mid \lambda \mid < 1$. This parameter can be used for predicting the stability behavior of the coupled aeroelastic system.

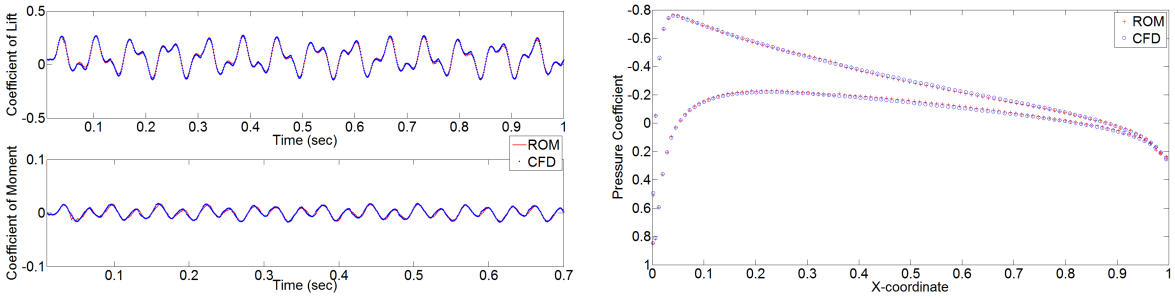

(a) Time history of lift and moment coefficient

(b) Surface pressure reconstruction

Figure 1: Reconstructions for a sinusoidal test signal obtained with ROM and inviscid CFD solver for 2-DoF airfoil at Mach 0.4

4 Results and prediction of flutter boundary

The formulated ROMs are employed for reconstruction of aerodynamic forces for 2-DoF NACA0012 airfoil. The ROM is trained for pitch and plunge frequencies of interest with chirp signals, which have high frequency content. For the basis of error analysis and in order to compare accuracy with different chirps, training frequencies for pitching and plunging motion are fixed. The models obtained thereafter are used to reconstruct test signals at these frequencies and an error analysis is performed to ascertain the optimum model order. Figure 1a shows one of the reconstructions of a test signal for an inviscid flow at Mach 0.4 obtained with an LPV-ARX model at a particular time instant. The ROM is also implemented to predict the surface pressure on the airfoil by considering 'surface-pressure' as the output of interest. Accurate surface pressure reconstructions (Figure 1b) for sinusoidal test signals are obtained at frequencies upto 35Hz with the ROM.

In Figure 2, normalised RMS error is shown, which is obtained by non-dimensionalising the RMS error with the maximum value of the quantity in the data-set. Both the ROMs perform well for frequencies upto 35Hz with a maximum normalised error of about 0.1. Chirps are used for building the ROMs with LPV-ARX model trained at Mach numbers of 0.3, 0.4 and 0.5. The reconstruction of coefficient of lift at Mach 0.4 shown in Figure 2a, shows slight better performance with the ARX model at lower plunge frequencies, while the moment reconstruction (Figure 2b) is in agreement for both the methods. From the error analysis, it is observed that both the models reported low normalised RMS values. Similar numerical studies by varying the mean pitch and plunge-amplitude of the airfoil are also performed, mostly for small perturbations. The ROMs performed well for such oscillations, which is suitable for linear stability analysis. In the current context, LPV-ARX model is the preferred choice as a single model can be used for different flow conditions. This is significant for performing uncertainty quantification. The formulated ROM is now used to predict flutter boundary of the system.

In the flutter analysis, the structural parameters for the airfoil are selected based on an experiment performed as part of the Benchmark Models Program (BMP)-NASA [14]. FSI simulations are also performed with a full inviscid aeroelastic solver for comparison with the ROM results. The predicted flutter boundary with the ROM shown in Figure 3 conforms well with the full order aeroelastic solution. There is some discrepancy with experimental results for lower Mach numbers, but nevertheless the accuracy of the ROM with respect to the aeroelastic solver is of primary interest and the ROM error is much smaller than other sources. This implementation is extremely cheap, e.g. run-time for the unsteady calculation shown in Figure 1a is in the

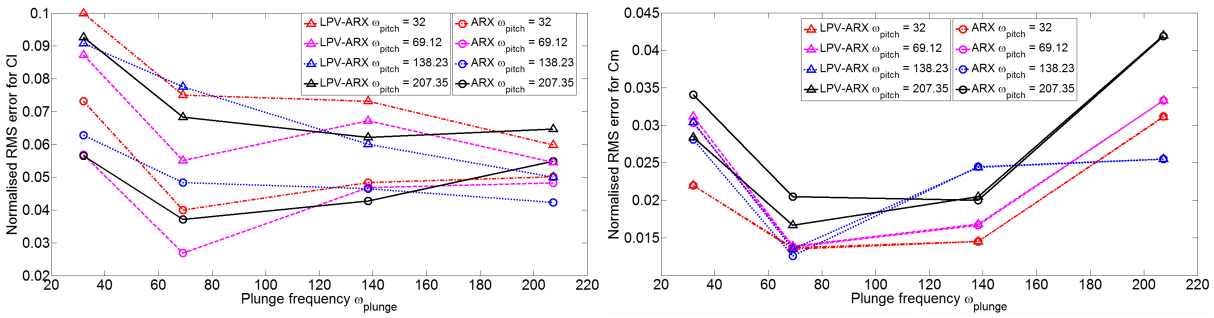

(a) Error estimates for lift coefficient

(b) Error estimates for moment coefficient

Figure 2: Comparison of errors in reconstruction of test signals at Mach 0.4 with ARX and LPV-ARX models

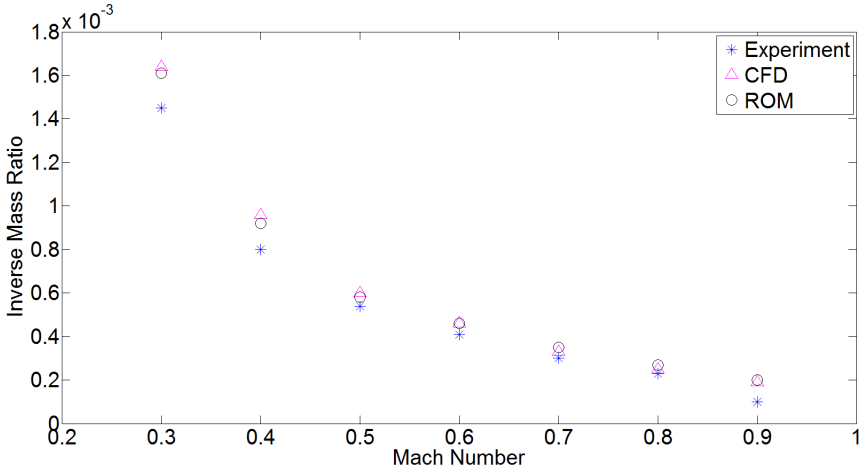

Figure 3: Comparison of predicted flutter boundary with ROM, FLUENT and experiment[14]

.

order of few seconds with the ROM, which is a significant gain over the unsteady CFD solver. During uncertainty quantification, this ROM is vital for performing cheap computations.

5 Uncertainty Quantification (UQ) with ROM

UQ of the stability behavior of aeroelastic systems is an important and significant problem for research. The structural and aerodynamic uncertainty needs to be accounted for obtaining reasonable estimates of the flutter boundary. This process is mostly computationally intractable with a high fidelity solver. We utilize the cheap aeroelastic solver formulated in the previous sections for performing UQ. The pitching stiffness k_α, plunging stiffness k_h and the distance between the elastic axis and the mass center x_α are assumed to be uncertain parameters. The input uncertainty is propagated by brute-force Monte-Carlo using 10000 samples. Normal, uniform and beta distributions are considered as probability density functions for the input parameters. The mean values of k_α, k_h and x_α are 4.83kN-m/rad, 47.66kN/m and 0 respectively. Three different values for standard deviation are considered for each of the distributions. Percentage variations of 1%, 5% and 10% are assumed, e.g. 10% variation in a quantity x for standard deviation σ is calculated as: $3\sigma = 10\%x$. The standard deviation with 10% variation for k_α, k_h and x_α is 0.161kN-m/rad, 1.59kN/m and 0.01355 respectively for each probability density

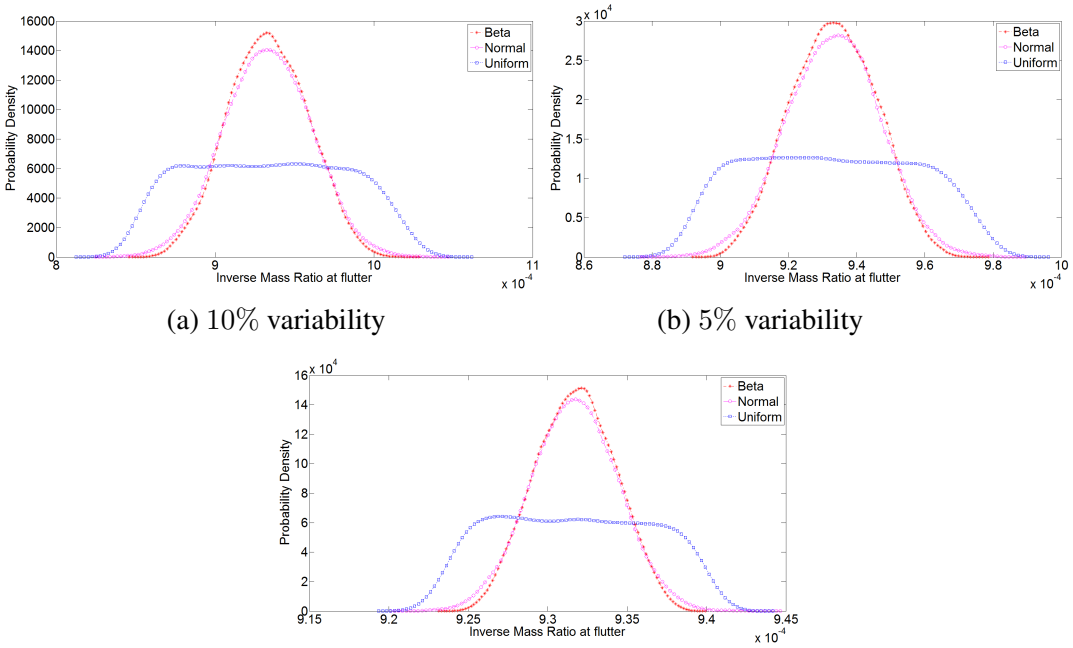

(a) 10% variability

(b) 5% variability

(c) 1% variability

Figure 4: Probabilistic distributions for inverse mass ratio at flutter (output) for Mach 0.4 considering normal, uniform and beta distributions under different input standard deviations

Distribution	$\mu * 10^{-3}$			$\sigma * 10^{-3}$		
	1%	5%	10%	1%	5%	10%
Normal	0.9317	0.9333	0.9332	0.0027	0.0137	0.0273
Beta	0.9318	0.9333	0.9336	0.0025	0.0124	0.0248
Uniform	0.9317	0.9327	0.9334	0.0048	0.0237	0.0474

Table 1: Estimated probability measures of mean μ and standard deviation σ for inverse mass ratio at flutter point for Mach 0.4 considering the input uncertainties

function. For the beta-distribution, parameter values used are $\alpha = \beta = 5$. Figure 4 shows the distribution of inverse mass ratio at flutter point for Mach 0.4.

The probabilistic measures of the inverse mass ratio at flutter for Mach 0.4 are summarized in Table 1 in terms of mean and standard deviation in the output. A lower standard deviation in the output is observed for less variability in the input parameters, which is expected. Error bars in the output of interest after taking into account the assumed structural uncertainties are shown in Figure 5. Error bars are drawn for $3 - \sigma$ limits obtained from Table 1 for inverse mass ratio at flutter for Mach 0.4. Some overlap with the experimental results is observed when a uniform distribution with 10% variability is assumed for the input parameters. This procedure can be effectively implemented for estimating uncertainties cheaply.

6 Conclusion

In this paper, we present an efficient method for predicting uncertainty in instability for aeroelastic systems. Computational FSI can be realized only if the simulation time for the flow solver is reduced. System identification based ROM can be an effective technique for approximating unsteady behaviour cheaply. The ROM is able to reconstruct aerodynamic time

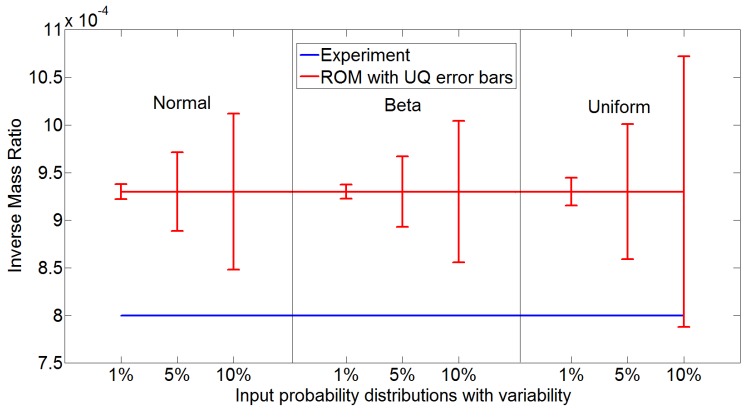

Figure 5: Error bars with 3-σ limits of uncertainty in inverse mass ratio at flutter for Mach 0.4 considering normal, beta and uniform distributions for input parameters with 1%, 5% and 10% variability

.

histories accurately. Further this ROM is employed for predicting stability boundaries. The ROM reconstructs results from the CFD solver accurately, though there is some discrepancy with respect to experimental results. But the trend is well reproduced with the solver. UQ is also performed with 3 uncertain structural parameters. The uncertainty is propagated using brute force Monte-Carlo to obtain probability distributions for flutter density. Further work involves extension of this method for analysing 3-D systems such as aircraft wings and wind turbines.

REFERENCES

[1] K. Carlberg, C. Farhat, J. Cortial, D. Amsallem, The GNAT method for nonlinear model reduction: Effective implementation and application to computational fluid dynamics and turbulent flows. *Journal of Computational Physics*, **242**, No. 1, 623–647, 2013.

[2] L. Ljung, *System Identification: Theory for the user, 2nd Edition*. Prentice-Hall, 1–8, 1987.

[3] D.E. Raveh, Identification of Computational-Fluid-Dynamics Based Unsteady Aerodynamic Models for Aeroelastic Analysis. *Journal of Aircraft*, **41**, No. 3, 620–632, 2004.

[4] K.K. Gupta, C. Bach, Systems Identification Approach for a Computational-Fluid-Dynamics-Based Aeroelastic Analysis. *AIAA Journal*, **45**, No. 12, 2820–2827, 2007.

[5] T.J. Cowan, A.S. Arena, Jr., K.K. Gupta, Accelerating CFD-based aeroelastic predictions using system identification, *AIAA-98-4152*, 1998.

[6] G.J. Balas, Linear Parameter-Varying Control and its Application to a Turbofan Engine. *International Journal of Robust and Nonlinear Control*, **12**, 763–796, 2002.

[7] A.A. Bachnas, Linear Parameter Varying Modeling of a High-Purity Distillation Column. *M.Sc Thesis*, Delft University of Technology, 2012.

[8] F.D. Bianchi, H. De Battista, R.J. Mantz, *Wind Turbine Control Systems Principles, Wind Turbine Control Systems - Principles, Modelling and Gain Scheduling Design, 1st Edition*. Springer, 2007.

[9] L.H. Lee, L.H., K. Poolla, 1997, Identifiability issues for parameter varying and multidimensional linear systems. *Proceedings of DETC*, California, 1997.

[10] M. Corno, J.-W. van Wingerden, M. Verhaegen, Linear Parameter-Varying System Identification: The Subspace Approach. *in Identification for Automotive Systems*, LNCIS 418, 53–65, 2012.

[11] B. Bamieh, L. Giarre, Identification of linear parameter varying models. *Proceedings of the 38th IEEE Conference on Decision and Control*, 1505–1510, Arizona, 1999.

[12] B. Bamieh, L. Giarre, Identification of linear parameter varying models. *International Journal of Robust and Non-linear Control*, **12**, 841–853, 2002.

[13] R.L. Harder, R.N. Desmarais, Interpolation using surface splines. *Journal of Aircraft*, **9**, No. 2, 189–191, 1972.

[14] J.A. Rivera, Jr., B.E. Dansberry, R.M. Bennett, M.H. Durham, W.A. Silva, NACA 0012 benchmark model experimental flutter results with unsteady pressure distributions. *AIAA-92-2396-CP*, 1992.